

# Classification of single voxel <sup>1</sup>H spectra of brain tumours using LCMoel

F. Raschke<sup>1</sup>, E. Fuster-Garcia<sup>2,3</sup>, K. S. Opstad<sup>1</sup>, and F. A. Howe<sup>1</sup>

<sup>1</sup>Division of Clinical Science, St George's University of London, London, United Kingdom, <sup>2</sup>IBIME and ITACA, Universidad Polit cnica de Valencia, Valencia, Spain, <sup>3</sup>Universitat Internacional Valenciana, Valencia, Spain

**Introduction:** <sup>1</sup>H MRS can determine a metabolic profile from brain tumours *in vivo* that has potential to aid their diagnosis and classification for improving treatment strategies. Pattern recognition methods have been used to automatically and objectively analyse <sup>1</sup>H spectra and typically show accuracies between 87% and 94% in classifying the most common tumour types: high-grade glioma (HGG), low-grade glioma (LGG) and meningioma (MNG) [1-4]. *LCMoel* is a widely used analysis tool originally designed to fit linear combinations of individual metabolite spectra to an *in vivo* <sup>1</sup>H spectrum [5]. In this study we present a simple tumour classification method without the need for implementation of pattern recognition by using *LCMoel* to fit mean spectra (*M*) of different tumour types instead of individual metabolite spectra. To account for tumour heterogeneity, a variability term (*V*) is calculated for each tumour type and added into the analysis. An average spectrum and variability term for normal white matter (NWM) are also included to account for partial volume effects with normal brain and to allow a mixed tissue analysis. *LCMoel* is then used to give an estimate of the proportion of each tissue type in a tumour spectrum and the highest tumour proportion used as a classifier. The *LCMoel* classification results are compared to that using the *Interpret Decision Support System (IDSS)* [4], which incorporates pattern recognition derived from correlation analysis and linear discriminant analysis, to classify brain tumour <sup>1</sup>H spectra.

**Methods:** **Data acquisition** 76 single voxel (SV) spectra (PRESS localization, TE = 30 ms, TR = 2000 ms) acquired from adult brain tumours at St George's on a 1.5 T Signa Horizon (GE Medical Systems, Milwaukee, WI, USA) during the *INTERPRET* and *eTUMOUR* projects (validated by an expert spectroscopist panel and histopathological diagnosis [6]) were divided into three major classes: 32 HGG (32 glioblastoma multiforme); 25 LGG (3 fibrillary astrocytomas; 9 diffuse astrocytomas, 4 gemistocytic astrocytomas, 3 oligoastrocytomas, 3 oligodendrogliomas) and 19 MNG. 11 spectra from NWM of healthy volunteers were acquired separately. **Data preparation** The three tumour datasets were divided into training and test sets using the Kennard and Stone algorithm (KSA) [7] to select tumour subsets of 10 spectra each. The KSA provides an optimum training set representation of *M* and *V* of the tumour datasets. Spectra were pre-processed (apodizing, phasing, referencing to choline peak at 3.2 ppm, truncating 4.0 ppm to 0.2 ppm and normalizing by setting the area under each spectrum over this limited ppm range to unity) and used to calculate the *M* and *V* terms from the three tumour training sets and 11 NWM spectra using PCA. To restrict *LCMoel* to only use the variability spectrum *V* of each tissue class with the appropriate main spectrum *M*, "soft constraints" are set in the *LCMoel* control parameters that define proportions used for the initial *LCMoel* analysis. A Cram r-Rao Lower Bound (CRLB) of ≤ 20% was used as a cut-off criterion for accepting an *LCMoel* output of *M* and *V* as a true component of the whole spectrum.

**Results:** Figure 1 shows the *M* and *V* components and variability for the four tissue types as calculated from the training sets. Similar variability patterns were obtained for the test set of 46 tumour spectra (22 HGG, 15 LGG and 9 MNG). The *LCMoel* residuals of the test set spectra fitted to *M* and *V* from the training set were close to the noise level. Table 1 compares the classification of the training and test set spectra using the direct *LCMoel* output and the *IDSS* classification output. The majority of mis-classified spectra were the same for both the *LCMoel* and *IDSS* analysis.

(No. of spectra)	training set					test set			
	HGG (10)	LGG (10)	MNG (10)	NWM (11)	Ø (41)	HGG (22)	LGG (15)	MNG (9)	Ø (46)
<i>LCModel</i>	80%	90%	90%	91%	<b>88%</b>	91%	87%	100%	<b>93%</b>
<i>IDSS</i>	80%	70%	90%	-	<b>80%</b>	86%	100%	100%	<b>95%</b>

Table 1

**Discussion:** We have shown proof-of-principle that *LCMoel* can be used as a direct classifier for brain tumour <sup>1</sup>H spectra by fitting representations of whole spectra for each tissue type. The accuracy of differentiating HGG, LGG and MNG using *LCMoel* compared well with the accuracy achieved with the *IDSS*. In the tissue compositions estimated by *LCMoel* we observed NWM contributions in LGG spectra and LGG contributions in MNG spectra. Further refinements are needed to ensure these additionally fitted tissue types represent a real tissue proportion, which could be the case for NWM spectra contribution to LGG spectra, and are not accounting for the limited representation of the tumour spectra, artefacts and noise as is probably the case for the LGG spectral components found in MNG. A reliable characterisation of the individual components in a mixed tissue spectrum would be valuable to classify MR spectra by the highest grade component fitted, as done for pathological analysis of a biopsy [8], and for analysis of MRSI data at tumour-brain boundaries. Further work is now needed to assess the analysis with larger data sets other tumour types and investigate what refinements can be made to the *LCMoel* basis set definitions and selection of training set spectra that may improve classification.

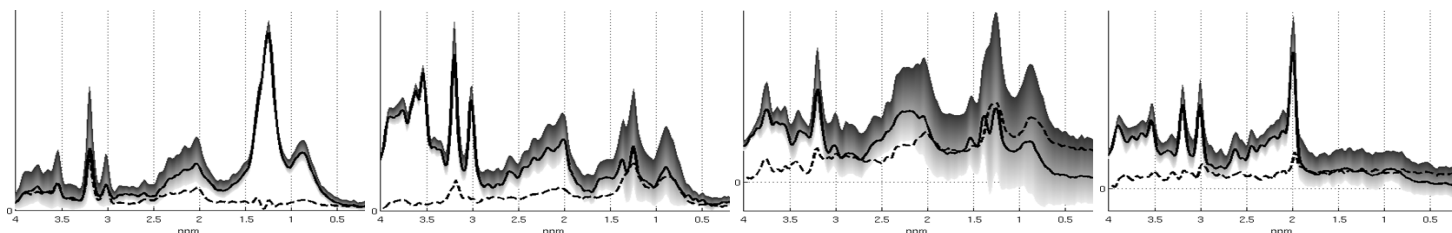


Figure 1: The mean *M* (solid line) and variability term *V* (dotted line) and resulting range (shaded area) of allowed spectra as defined by the *LCMoel* 'soft constraints' for the tissue classes HGG, LGG, MNG and NWM (in order from left to right).

## References

[1] Opstad KS et al. *NMR Biomed* 20:763-770; 2007. [2] Devos A et al. *J Magn Reson* 170:164-175; 2004. [3] Garc a-G mez J et al. *Magn Reson Mater Phys Biol Med* 22:5-18; 2009. [4] Tate AR et al. *NMR Biomed* 19:411-434; 2006. [5] Provencher SW *Magn Reson Med* 30:672-679; 1993. [6] van der Graaf M *NMR Biomed* 21:148-158; 2008. [7] Kennard RW and Stone LA *Technometrics* 11:137-148; 1969. [8] Louis D *Acta Neuropathol* 114:97-109; 2007.

## Acknowledgements

This work is funded by CRUK & ESRC Cancer Imaging Programme at the Children Cancer and Leukaemia Group (CCLG), in association with the MRC and Dept of Health (England), Grant C7809/A10342. Data was collected as part of the EU funded *INTERPRET* and *eTUMOUR* projects.